

with crystals of both emerging simultaneously from the same solution. The tetragonal form would imply rapid interconversion of N-H tautomers or stacking disorder in the crystal.¹⁴ Thus, it seems as if the presence of an impurity such as Ag(II) can induce one or the other of these, which ultimately leads to effectively four-fold symmetry. It is possible, therefore, that the Cu(II)

(14) M. J. Hamor, T. A. Hamor, and J. L. Hoard, *J. Amer. Chem. Soc.*, **86**, 1938 (1964).

impurity in the W & F crystals of porphine might also be effective in this connection in a monoclinic case.

Acknowledgment. We would like to take the opportunity here to gratefully acknowledge the support of this work by the National Science Foundation, Molecular Biology Section (Grants GB-5686, GB-7399, and GB-15402). In addition, we would like to thank Mr. Richard L. Vandlen for the many ways he has contributed to all aspects of this work.

Structure of Tetra-*n*-propylporphine. An Average Structure for the Free Base Macrocycle from Three Independent Determinations

Penelope W. Coddling¹ and A. Tulinsky*

Contribution from the Departments of Chemistry and Biochemistry, Michigan State University, East Lansing, Michigan 48823. Received September 18, 1971

Abstract: The crystal and molecular structure of $\alpha,\beta,\gamma,\delta$ -tetra-*n*-propylporphine has been solved using X-ray crystallographic techniques. The structure was solved using Sayre's equation. The molecule is centrosymmetric with two independent pyrrole rings. A common structure for the free base macrocycle was obtained by averaging from the tetraphenylporphine, porphine, and tetrapropylporphine determinations. The free base structure consists of opposite pyrrole rings possessing imino hydrogen atoms and the pyrrole rings differing in like pairs. Small differences which are localized at the bridge carbon atoms were found for the substituted compounds. In addition, the aliphatic substituent seems to decrease some of the differences between the two pyrrole rings. The individual pyrrole rings are planar to ± 0.007 Å and the nucleus of the tetrapropylporphine ring is essentially planar (± 0.04 Å). Some small deviations from planarity are probably due to packing effects with the closest intermolecular distance being 3.36 Å. The propyl groups are in an extended configuration efficiently filling the space between molecules in the crystal.

From the X-ray crystallographic structure determinations of two synthetic free base porphyrins, triclinc tetraphenylporphine (TPP)² and porphine,³ there are indications that a common structure exists for the macrocyclic ring system of four alternate pyrrole rings joined by methine carbon atom bridges. This structure consists of opposite pyrrole rings possessing imino hydrogen atoms with small structural differences between these rings and the other two pyrrole rings (in bond distances and bond angles). At the time when this work was begun, the redetermination of the structure of porphine was not yet completed so that there were two main objectives in the structure determination of $\alpha,\beta,\gamma,\delta$ -tetra-*n*-propylporphine (TPrP): (1) to obtain an accurate structure of the free base macrocycle and (2) to try to determine the effect of an aliphatic substitution on the free base structure by comparing the structure of TPrP with that of TPP and porphine. Extensive studies of the visible spectra of porphyrins have shown that a correlation exists between the positions and relative intensities of the visible absorption bands and the nature of the side chains at various substitution positions on the macrocycle. These studies suggest that different changes in the π -electron density of the macrocycle are caused by different substituents.⁴

Since the electronic effects of an aromatic (TPP) and an aliphatic substitution (TPrP) are fairly different (Figure 1), under favorable circumstances, a comparison of these two structures with that of porphine could lead to some insight concerning changes occurring in the π -electron density accompanying substitution of the porphine ring. The extent to which this has been accomplished will be clear from the results to be reported here.

Experimental Section

Single crystals of TPrP in the form of purple hexagonal prisms were grown by slowly evaporating a saturated benzene solution of TPrP.⁵ A suitable crystal with approximate dimensions of 0.15 mm in all directions was selected for X-ray examination. Preliminary X-ray diffraction measurements showed the crystal to be monoclinic with unit cell dimensions of $a = 5.078$ (5), $b = 11.59$ (2), $c = 22.39$ (3) Å; $\beta = 99.50$ (5)°. Systematic absences fixed the space group to be $P2_1/c$. The calculated density of the crystal on the basis of two molecules per unit cell is 1.223 g cm⁻³ and the observed density measured by flotation in aqueous silver nitrate solution is 1.22 (1) g cm⁻³.

All the X-ray measurements and the intensity data collection were made with Cu K α radiation using a Picker four-circle automatic X-ray diffractometer controlled by a Ditigal Equipment Corp. (DEC) 4K PDP-8 computer (FACS-I System) coupled to a DEC 32K

(1) NDEA Title IV Fellow, 1969-1971.

(2) S. J. Silvers and A. Tulinsky, *J. Amer. Chem. Soc.*, **89**, 3331 (1967).

(3) B. M. L. Chen and A. Tulinsky, *ibid.*, **94**, 4144 (1972).

(4) For a review of spectral studies of porphyrins, see J. E. Falk, "Porphyrins and Metalloporphyrins," Elsevier, Amsterdam, 1964, Chapter 6.

(5) We would like to thank Dr. Alan D. Adler of the New England Institute for kindly supplying us with a sample of TPrP.

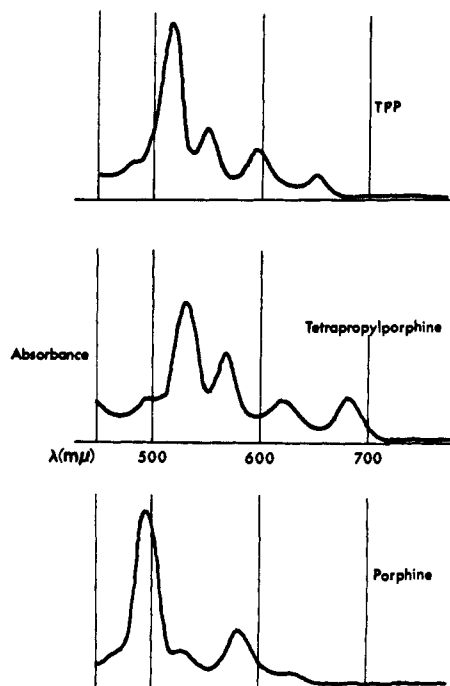


Figure 1. Visible absorption spectra of tetraphenylporphine, tetrapropylporphine, and porphine. The solvent for all three was benzene.

disk file. Intensities of reflections were measured under the control of a computer program using a "wandering" ω -step-scan procedure which also utilized balanced Ni/Co filters.⁶ The step-scan was performed in 0.03° increments of the most sensitive angular position (ω) and extended $\pm 0.075^\circ$ from the calculated peak position. Each intensity was measured for a preset constant time count of 4 sec at each step and the four largest successive measurements were totalled to give the intensity of the reflection (count 6-drop 2).⁷ The background was measured with a Co filter at the ω value of the step with the largest intensity for a 4-sec count and this measurement was multiplied by four to give the total background intensity. When the calculated ω value did not correspond exactly to the observed peak position of a reflection, an additional step or two were taken to assure maximum intensity for the reflection. Throughout the intensity data collection, the alignment of the crystal was continually monitored and could be automatically "realigned" if necessary by the computer program.⁸ However, the alignment of the crystal proved to be sufficiently stable through data collection so as not to require realignment. Finally, since the step-scan procedure is essentially a stationary crystal-stationary counter technique, in order to avoid $K\alpha$ splitting effects, the data collection was confined to $\sin \theta/\lambda < 0.55$, which corresponds to minimum d spacings of approximately 0.94 \AA .

Before intensity data collection was undertaken, the mosaic spreads of a number of reflections suitably distributed in reciprocal space were measured to ensure the crystal quality and to aid in the selection of the quadrant of reciprocal space to be used for intensity data collection. The mosaic spreads were symmetrical and single peaked and had widths of less than 0.3° in ω from background to background. Therefore, the choice of the data collection quadrant was decided on the basis of convenience.

Throughout the intensity data collection, the intensities of three reflections defining the alignment of the crystal were measured at regular intervals (the $(20\bar{2})$ reflections at $\chi = 90^\circ$ at two ϕ values about 90° apart; and the (060) reflection at $\chi = 0^\circ$). The monitored reflections were measured 22 times over approximately a 20-hr period and the per cent standard deviations from average intensities were 1.0, 0.9, and 0.5%, respectively. Thus, there was no intensity

loss due to X-ray exposure and the crystal remained well aligned throughout the data collection.

Due to the practically isotropic shape of the crystal and to its small linear absorption coefficient ($\mu = 9.11 \text{ cm}^{-1}$), little variation of intensity was observed with azimuthal angle (ϕ) for $\chi = 90^\circ$ reflections. Consequently, a correction for absorption was not applied.

In all, the intensities of 1744 independent reflections were surveyed. A redundant set of $(0kl)$ reflections was measured and used to calculate $R_{\text{obsd}} = 2(\sum |I(0kl)| - I(0k\bar{l}) / \sum (I(0kl) + I(0k\bar{l})))$. The excellent degree of reproducibility of the data is indicated by the value of $R_{\text{obsd}} = 0.011$ for the 382 redundant reflections. The average value of the measured intensity of $(h0l)$ systematically absent reflections was used to fix a lower observable limit. This limit gave 331 accidentally absent reflections in the data set and 1413 (81%) observable reflections. These intensities were then converted to relative structure amplitudes by application of Lorentz and polarization factors (L_p).

Structure Analysis

The structure amplitudes were converted to normalized values ($|E|$'s) using an approximate absolute scale and an average temperature factor of 3.5 \AA^2 determined by Wilson's method.⁸ The statistical distribution of the normalized structure factors along with the theoretical distributions for the centric and acentric cases is given in Table I, where the normalized struc-

Table I. Statistical Distribution of $|E|$'s

| | TPrP | Theoretical | |
|-----------------------------|-------|-------------|----------|
| | | Centric | Acentric |
| $\langle E \rangle$ | 0.83 | 0.80 | 0.89 |
| $\langle E^2 \rangle$ | 1.00 | 1.00 | 1.00 |
| $\langle E^2 - 1 \rangle$ | 0.90 | 0.97 | 0.74 |
| % > 1.0 | 31.08 | 32.00 | 37.00 |
| % > 2.0 | 3.66 | 5.00 | 1.80 |
| % > 3.0 | 0.50 | 0.30 | 0.01 |

ture factors were scaled such that $\langle E^2 \rangle = 1.0$. As expected, it can be seen from Table I that the distribution of $|E|$'s for TPrP is similar to the distribution for a centrosymmetrical crystal.

The phases of the largest $|E|$'s were obtained by reiteratively applying Sayre's equation: $\text{sign}(E_n) = \text{sign}(\sum_k E_k E_{n-k})$. Based on a ratio of [(number of signs)/atom] ~ 10 , the 202 $|E|$'s with values greater than 1.3 were used in a sign determination computer program.⁹ All 202 phases were determined and an E map using these phases revealed the positions of all the nonhydrogen atoms. This trial structure was then used to calculate structure factors employing an average isotropic thermal parameter for all the atoms; the R factor for this calculation was 0.31, $R = \sum ||F_o| - |F_c|| / \sum |F_o|$. The additional signs obtained in this manner (total of 1100) and their observed structure amplitudes were used to calculate an electron density from which estimates of individual thermal parameters and improved atomic positions were obtained.

Full-matrix, unit weight least-squares refinement was initiated at this stage utilizing individual isotropic thermal parameters.¹⁰ Three cycles of refinement, one varying the coordinates of the ten atoms of the two pyrrole rings, another varying coordinates of the eight

(6) R. L. Vandlen and A. Tulinsky, *Acta Crystallogr., Sect. B*, **27**, 437 (1971).

(7) H. W. Wyckoff, M. Doscher, D. Tsernoglou, T. Inagami, L. N. Johnson, K. D. Hardman, N. M. Allewell, D. M. Kelly, and F. M. Richards, *J. Mol. Biol.*, **27**, 563 (1967).

(8) A. J. C. Wilson, *Nature (London)*, **150**, 151 (1942).

(9) R. E. Long, Ph.D. Thesis, University of California, Los Angeles, Calif., 1965.

(10) Scattering factors for carbon and nitrogen atoms were taken from D. J. Cromer and J. T. Waber, *Acta Crystallogr.*, **18**, 104 (1965).

atoms of the bridge positions and propyl side chains, and the last varying all the isotropic thermal parameters, reduced R to 0.150. At this stage, anisotropic thermal parameters were introduced into the refinement and the unit weight weighting scheme was replaced with a Hughes-type weighting scheme given in Table II.¹¹

Table II. Weighting Scheme for TPrP Least-Squares Refinement^a

| | |
|-----------------------|--|
| $I > 20,000$ | $\omega = (20,000/I) \times 1/(0.04 F_o)^2$ |
| $500 < I \leq 20,000$ | $\omega = 1/(0.04 F_o)^2$ |
| $15 < I \leq 500$ | $\omega = 1/(\% \text{ error} \times F_o)^2$ |

^a The per cent error curve was constructed to be similar to that used with the porphine data,³ with limits of 100% error for $I = 15$, and 4% error for $I = 500$ counts/16 sec.

The anisotropic thermal parameters were varied for six atoms per cycle, two cycles with respect to the atoms of one pyrrole ring and one methine carbon atom, and the last cycle varied the β_{ij} 's of the six propyl carbon atoms. After refining the thermal parameters and coordinates of the asymmetric unit one time, the R factor decreased to 0.135.

A difference Fourier synthesis was then computed revealing the positions of all the hydrogen atoms clearly except that of the imino hydrogen atom. The imino hydrogen was obscured at this time by residual densities present on the nitrogen atoms and a relatively large positive peak near the center of symmetry.¹² The hydrogen atoms were assigned isotropic thermal parameters which were 25% greater than the thermal parameters of the atoms to which they were bonded and they were included into the refinement.¹³ The structure was then refined by alternating full cycles of refinement on the carbon and nitrogen atom parameters with cycles of refinement on the hydrogen atom coordinates and R decreased to 0.089.

At this stage, it was clear that 13 of the largest low-order reflections which showed marked discrepancies between $|F_o|$ and $|F_c|$ were affected by extinction. They were corrected for secondary extinction using an isotropic extinction coefficient, g , which was determined to be $4.58 \times 10^{-7} \text{ e}^{-2}$ from the slope of a plot of I_c/I_o vs. I_c ;¹⁴ the corrected structure amplitudes were then obtained from $F_{\text{corr}}^2 = F_o^2(1 + 2g(L_p)F_c^2)$ and they are listed in Table III along with other pertinent quantities.

A structure factor calculation including the corrected values for the 13 extinction affected reflections produced an R factor of 0.080. A difference Fourier synthesis at this time revealed the position of the imino hydrogen atom to be associated with one of the pyrrole rings; this atom was then included in the refinement similarly to other hydrogen atoms. The structure was refined as previously for several cycles and the resulting R factor was 0.065.

(11) E. W. Hughes, *J. Amer. Chem. Soc.*, **63**, 1737 (1941).

(12) This peak has persisted throughout the refinement at about 0.7 e Å⁻³ near the center of symmetry. In this space group, the standard deviation at this position is $\times \sqrt{2}$ the standard deviation expected at general positions.

(13) A spherical hydrogen atom scattering factor was taken from R. F. Stewart, E. R. Davidson, and W. T. Simpson, *J. Chem. Phys.*, **42**, 3175 (1965).

(14) R. W. James, "The Optical Principles of the Diffraction of X-Rays," G. Bell and Sons Ltd., London, 1950, pp 292-294.

Table III. Reflections Corrected for Extinction

| hkl | $ F_o $ | $ F_{\text{corr}} $ | $ F_c ^a$ |
|--------------|---------|---------------------|-----------|
| 020 | 284 | 334 | 333 |
| 01 $\bar{1}$ | 192 | 218 | 215 |
| 002 | 273 | 382 | 377 |
| 02 $\bar{2}$ | 180 | 206 | 202 |
| 01 $\bar{5}$ | 281 | 318 | 330 |
| 11 $\bar{1}$ | 196 | 209 | 220 |
| 10 $\bar{2}$ | 215 | 234 | 246 |
| 112 | 449 | 609 | 599 |
| 113 | 292 | 323 | 326 |
| 104 | 423 | 527 | 527 |
| 114 | 372 | 434 | 437 |
| 11 $\bar{4}$ | 189 | 198 | 202 |
| 116 | 312 | 329 | 338 |

^a $|F_c|$ taken from final structure factor calculation (at $R = 0.054$).

A calculation of the bond distances based on the coordinates of this structure showed certain anomalies: the C-C distances in the propyl groups ranged from 1.492 to 1.526 Å, considerably shorter than the expected distance of about 1.54 Å; the bond distances of the pyrrole rings were within 0.01-0.02 Å of the expected values but the exact nature of the geometry of the rings was not evident. The apparent shortening of the propyl group distances suggested that perhaps the early introduction of the hydrogen atoms into the structure factor calculations and the subsequent refinement of their coordinates might have prejudiced the least-squares analysis as has been observed in the structure determination of $\alpha, \beta, \gamma, \delta$ -tetra(4-pyridyl)porphinatomonopyridinezinc(II) (PyZnTPyP).¹⁵ In the PyZnTPyP structure analysis, the least-squares refinement was carried out in two parts: refinement I excluded hydrogen atoms completely from the structure, and refinement II included hydrogen atoms in structure factor calculations and subsequently in the refinement. A comparison of the two resulting structures showed that refinement II had produced systematic shifts in the positions of the carbon atoms bonded to hydrogen atoms with the cumulative result of "shrinking" the rings containing these carbon atoms. To test the possibility of a similar kind of occurrence in the propyl groups of TPrP, the propyl hydrogen atoms were removed from the structure for which R was 0.065 and one full cycle of refinement on the carbon and nitrogen atom parameters was carried out which decreased R from 0.108 to 0.105. The resulting structure had longer propyl group distances and slight changes in the pyrrole distances.

In addition to the foregoing anomalies, the final R factor of 0.065 seemed large with respect to the reproducibility observed with the redundant reflection measurements ($R_{\text{obsd}} = 0.011$). This prompted the examination of the weighted differences between $|F_o|$ and $|F_c|$, which indicated that the weighting scheme as given in Table II was probably too severe for smaller structure amplitudes. This effect can be seen from the comparison of a plot of the ratio $\langle \Delta F \rangle / \langle |F_o| \rangle$ vs. $\langle |F_o| \rangle$, where $\Delta F = ||F_o| - |F_c||$, with that of the $\sigma|F_o|$ vs. $\langle |F_o| \rangle$ curve of the original weighting scheme (Figure 2). From Figure 2, it can be seen that the error in the measurement of the small intensities was severely overestimated in the assumed per cent error curve of the

(15) D. M. Collins and J. L. Hoard, *J. Amer. Chem. Soc.*, **92**, 3761 (1970).

Table IV. Final Atomic Parameters, Carbon and Nitrogen^a

| Atom | <i>x</i> | <i>y</i> | <i>z</i> | β_{11} | β_{22} | β_{33} | β_{12} | β_{13} | β_{23} | Peak height, e Å ⁻³ |
|----------------------|------------|-------------|------------|--------------|--------------|--------------|--------------|--------------|--------------|--------------------------------|
| NA | 0.7655 (5) | -0.0206 (2) | 0.5669 (1) | 0.0523 | 0.0098 | 0.0022 | -0.0004 | 0.0026 | -0.00010 | 7.8 |
| CA1 | 0.7425 (6) | -0.1215 (3) | 0.5982 (1) | 0.0496 | 0.0101 | 0.0020 | -0.0029 | 0.0021 | 0.00005 | 6.2 |
| CA2 | 0.5571 (7) | -0.0980 (3) | 0.6388 (1) | 0.0613 | 0.0113 | 0.0024 | -0.0033 | 0.0034 | 0.00004 | 5.4 |
| CA3 | 0.4728 (6) | 0.0124 (3) | 0.6308 (1) | 0.0545 | 0.0122 | 0.0025 | -0.0013 | 0.0034 | -0.00046 | 5.8 |
| CA4 | 0.6048 (6) | 0.0628 (3) | 0.5852 (1) | 0.0439 | 0.0103 | 0.0021 | 0.0001 | 0.0018 | -0.00041 | 6.4 |
| CM5 | 0.5785 (6) | 0.1767 (3) | 0.5649 (1) | 0.0436 | 0.0104 | 0.0021 | 0.0012 | 0.0011 | -0.00047 | 6.0 |
| NB | 0.8820 (5) | 0.1683 (2) | 0.4892 (1) | 0.0473 | 0.0093 | 0.0020 | -0.0003 | 0.0016 | 0.00004 | 7.3 |
| CB1 | 0.7127 (6) | 0.2248 (3) | 0.5211 (1) | 0.0489 | 0.0090 | 0.0022 | 0.0017 | 0.0004 | 0.00002 | 5.8 |
| CB2 | 0.6944 (7) | 0.3443 (3) | 0.5033 (1) | 0.0666 | 0.0107 | 0.0027 | 0.0051 | 0.0024 | 0.00016 | 5.3 |
| CB3 | 0.8479 (7) | 0.3587 (3) | 0.4605 (1) | 0.0673 | 0.0093 | 0.0028 | 0.0025 | 0.0021 | 0.00052 | 5.0 |
| CB4 | 0.9637 (6) | 0.2478 (3) | 0.4509 (1) | 0.0491 | 0.0093 | 0.0022 | 0.0000 | 0.0007 | 0.00003 | 5.6 |
| CM6 | 1.1338 (6) | 0.2264 (3) | 0.4090 (1) | 0.0521 | 0.0092 | 0.0022 | -0.0014 | 0.0014 | 0.00026 | 5.4 |
| CP51 | 0.3943 (6) | 0.2539 (3) | 0.5941 (1) | 0.0474 | 0.0114 | 0.0025 | 0.0036 | 0.0013 | -0.00080 | 5.4 |
| CP52 | 0.5346 (7) | 0.3133 (3) | 0.6513 (1) | 0.0559 | 0.0123 | 0.0028 | 0.0024 | 0.0017 | -0.00134 | 5.3 |
| CP53 | 0.3437 (8) | 0.3870 (3) | 0.6803 (2) | 0.0741 | 0.0143 | 0.0036 | 0.0056 | 0.0036 | -0.00160 | 4.7 |
| CP61 | 1.1840 (7) | 0.3223 (3) | 0.3657 (1) | 0.0627 | 0.0096 | 0.0026 | -0.0029 | 0.0024 | 0.00059 | 5.5 |
| CP62 | 0.9992 (7) | 0.3151 (3) | 0.3047 (1) | 0.0623 | 0.0114 | 0.0025 | -0.0020 | 0.0023 | 0.00086 | 5.2 |
| CP63 | 1.0848 (7) | 0.3988 (3) | 0.2586 (2) | 0.0745 | 0.0133 | 0.0029 | -0.0019 | 0.0021 | 0.00191 | 4.6 |
| $\sigma \times 10^6$ | 46-77 | 21-35 | 10-17 | 137-265 | 27-52 | 6-12 | 51-95 | 24-44 | 11-20 | |

^a Anisotropic temperature factor = $\exp[-(\beta_{11}h^2 + \beta_{22}k^2 + \beta_{33}l^2 + 2\beta_{12}hk + 2\beta_{13}hl + 2\beta_{23}kl)]$. Standard errors of coordinates in parentheses.

original weighting scheme. Therefore, it was decided to carry out the remainder of the least-squares refinement based upon a unit weight scheme.

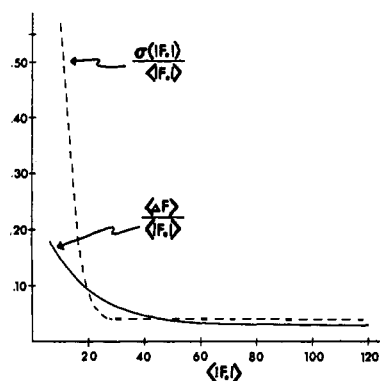


Figure 2. Comparison of Hughes-type weighting with unit weight scheme. Quantities are defined in the text.

The observed electron density based on phases obtained with the structure at $R = 0.105$ was used to obtain a new set of atomic positions. The positions for the carbon and nitrogen atoms were obtained by fitting the observed peaks with the Gaussian function¹⁶ given by

$$\rho = \exp(p - (1/2)rx^2 - (1/2)sy^2 - (1/2)tz^2 + ux + vy + wz + lxy + mxz + nyz)$$

The ten parameters (l, m, \dots, w) were determined by a least-squares fit of the values of the electron density, ρ , at 27 equally weighted grid points which were centered around the peak. The coefficients of the least-squares equations for this case are tabulated by Dawson.¹⁷ The position of the center is obtained from the three simultaneous equations for peak maxima in the x, y, z directions. Back shift corrections for nonconvergence

(16) D. P. Shoemaker, J. Donohue, V. Schomaker, and R. B. Corey, *J. Amer. Chem. Soc.*, **72**, 2328 (1950).

(17) B. Dawson, *Acta Crystallogr.*, **14**, 999 (1961).

of the Fourier series and other such effects were made using the Gaussian positions of the peaks from an identical density of the calculated structure. The positions of the hydrogen atoms were also obtained from Gaussian approximations to their peak shapes in the corresponding difference electron density map.

Three cycles of refinement, one on all the parameters of the carbon and nitrogen atoms, a second on the coordinates of all the hydrogen atoms, and a last cycle on the positional parameters of the nonhydrogen atoms, reduced the R factor from 0.062 to 0.054. Since the change between the last two cycles was only 0.001 in the R factor and the parameter shifts were insignificant with respect to the standard deviations of the coordinates, the refinement of the structure was terminated at this point.

Results¹⁸

The final atomic coordinates and anisotropic thermal parameters of the carbon and nitrogen atoms are listed in Table IV with the atoms labeled according to

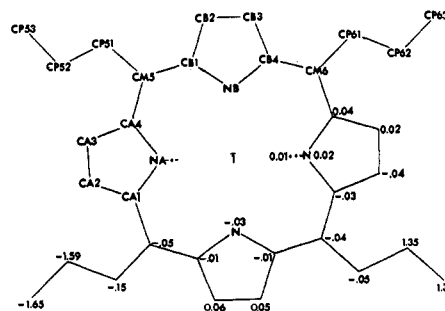


Figure 3. Numbering system of molecule (top); deviations (in ångströms) from nuclear least-squares plane (bottom).

Figure 3. The hydrogen atom coordinates and isotropic thermal parameters are given in Table V. The

(18) Copies of the observed and calculated structure amplitudes are available from one of the authors (A. T.) upon request.

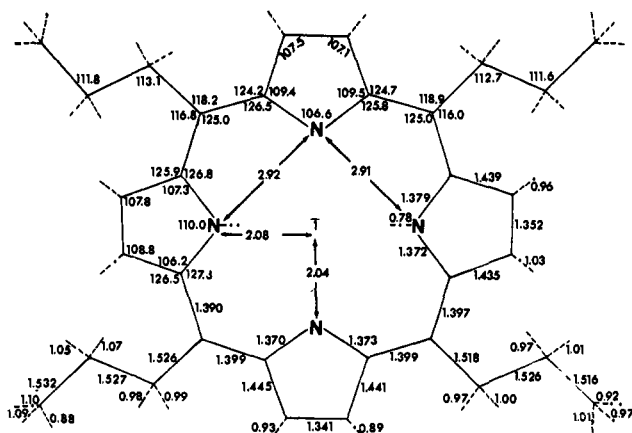


Figure 4. Interatomic distances (in ångströms) and bond angles (in degrees).

limits of the standard deviations obtained from the least-squares calculations are given in the last row of Tables IV and V.

Table V. Final Hydrogen Atom Parameters

| Atom | <i>x</i> | <i>y</i> | <i>z</i> | Isotropic <i>B</i> | Peak height, $e \text{ \AA}^{-3}$ |
|----------------------|----------|----------|----------|--------------------|-----------------------------------|
| HNA | 0.8548 | -0.0146 | 0.5420 | 4.5 | 0.4 |
| HA2 | 0.5026 | -0.1533 | 0.6668 | 5.6 | 0.4 |
| HA3 | 0.3390 | 0.0577 | 0.6515 | 5.5 | 0.5 |
| HB2 | 0.5911 | 0.3906 | 0.5209 | 5.8 | 0.5 |
| HB3 | 0.8845 | 0.4274 | 0.4423 | 5.6 | 0.5 |
| H51A | 0.3167 | 0.3136 | 0.5643 | 5.3 | 0.4 |
| H51B | 0.2438 | 0.2094 | 0.6034 | 5.3 | 0.4 |
| H52A | 0.6767 | 0.3593 | 0.6398 | 6.3 | 0.4 |
| H52B | 0.6005 | 0.2476 | 0.6796 | 6.3 | 0.4 |
| H53A | 0.4174 | 0.4276 | 0.7169 | 7.1 | 0.4 |
| H53B | 0.2552 | 0.4538 | 0.6534 | 7.1 | 0.3 |
| H53C | 0.1838 | 0.3541 | 0.6855 | 7.1 | 0.4 |
| H61A | 1.3736 | 0.3186 | 0.3598 | 5.6 | 0.4 |
| H61B | 1.1596 | 0.3968 | 0.3847 | 5.6 | 0.5 |
| H62A | 1.0051 | 0.2279 | 0.2888 | 5.7 | 0.4 |
| H62B | 0.8055 | 0.3353 | 0.3116 | 5.7 | 0.4 |
| H63A | 1.2899 | 0.3845 | 0.2524 | 6.5 | 0.4 |
| H63B | 0.9732 | 0.4016 | 0.2244 | 6.5 | 0.4 |
| H63C | 1.0901 | 0.4888 | 0.2735 | 6.5 | 0.4 |
| $\sigma \times 10^4$ | 64-78 | 29-35 | 14-18 | | |

A plane was fitted to the 24 carbon and nitrogen atoms of the nucleus of the TPrP molecule by the method of least squares (NLS). The deviations of the

Table VI. Atomic Deviations from the Least-Squares Plane of Individual Pyrrole Rings

| Pyrrole A | | Pyrrole B | |
|----------------------------------|--------|----------------------------------|--------|
| Na | +0.002 | NB | +0.010 |
| CA1 | -0.004 | CB1 | -0.007 |
| CA2 | +0.004 | CB2 | +0.002 |
| CA3 | -0.002 | CB3 | +0.004 |
| CA4 | +0.000 | CB4 | -0.008 |
| $\sigma = \pm 0.003 \text{ \AA}$ | | $\sigma = \pm 0.007 \text{ \AA}$ | |

atoms from this plane are shown in Figure 3. The deviations of the atoms from the least-squares plane of each pyrrole are listed in Table VI. An examination

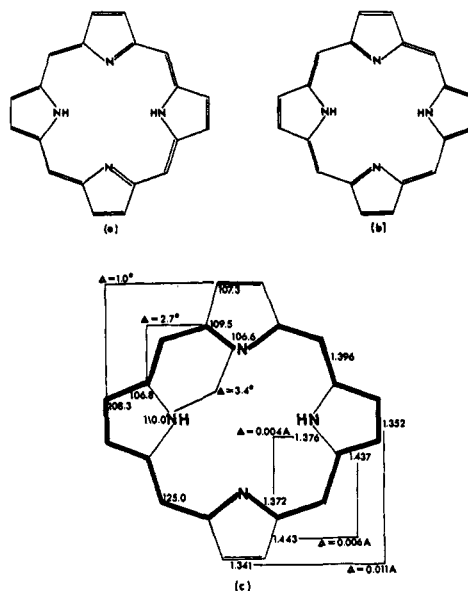


Figure 5. (a and b) Dominant resonance structures of porphine macrocycle; (c) average observed distances and angles of the independent pyrroles TPrP. Differences (Δ) between corresponding bonds and angles also shown; expected nature of hybrid of dominant resonance structures shown with heavy line and double bond representation.

of the deviations from the individual pyrrole planes shows that the rings are planar within $\pm 0.007 \text{ \AA}$ while the porphine nucleus of TPrP shows deviations of up to $\pm 0.04 \text{ \AA}$. The standard deviation of the latter is of the order of 0.015 \AA .

Interatomic distances and bond angles of TPrP are shown in Figure 4. The standard deviations of the bond lengths and bond angles for the carbon and nitrogen atoms are about $\pm 0.004 \text{ \AA}$ and $\pm 0.2-0.4^\circ$, respectively; these values are based on the standard deviations of the atomic coordinates in the final cycle of least-squares refinement.

Discussion of the Results

The presence of the imino hydrogen atom in the difference electron density with a peak height of $0.4 e \text{ \AA}^{-3}$ bound to the nitrogen atom of a pyrrole ring indicates that the TPrP has two like pairs of independent pyrrole rings similar to TPP² and porphine.³ The bond distances and bond angles in Figure 4 show additional small but significant differences between the two rings. The mean observed distances and bond angles of the independent pyrrole rings and the differences between the corresponding atoms involved are shown in Figure 5. As in the structures of TPP and porphine, these differences correspond approximately to those expected for a hybrid of the two major resonance forms of the macrocycle² shown in Figure 5 (a, b).

Since the structures of three different free base compounds (porphine, TPP, TPrP) show remarkably similar dimensions and geometry for the macrocyclic ring and since their determinations were carried out to comparable degrees of refinement ($R = 0.059, 0.056, 0.054$ for porphine, TPP, TPrP, respectively), these structures have been averaged to obtain a *general structure of the free base porphyrin macrocycle*. The three structure determinations provide four examples of each type of pyrrole ring; the mean distances and

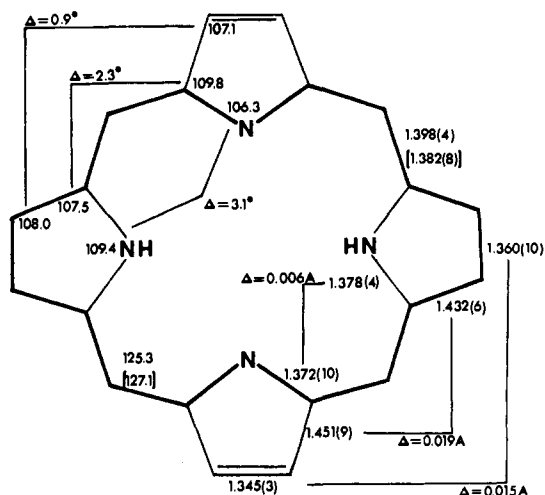


Figure 6. Average structure for free base porphine. Average obtained using TPP, porphine, and TPrP. Standard deviations of distances in parentheses; standard deviations of angles 0.3–0.7°. The average bridge distance and angle of porphine in brackets.

angles for these rings are shown in Figure 6. The standard deviations from the mean fluctuate from 0.003 to 0.010 Å for the bond lengths and from 0.3 to 0.7° for the bond angles and all of the observed distances and angles are within 2σ of the mean values. The largest differences among the three structures reside with the methine carbon atoms (C_m): the average C_α – C_m bond (where C_α is the pyrrole atom bonded to nitrogen) in the substituted compounds is 0.016 Å longer than the mean observed distance in porphine and the average C_α – C_m – C_α' bond angle is 1.8° smaller for the substituted compounds. The overall change produced by these differences is a slight increase in the size of the interior of the porphine ring; the distance between the bridge carbon atom and the center of the ring is increased by about 0.02 Å in the substituted compounds. Since these are the largest differences observed among the three structure determinations, they suggest that substitution at the bridge carbon atom produces some localized changes in the π -electron density but that the general macrocyclic structure remains essentially intact.

Although the three structures for the free base macrocycle are very similar, some small but significant differences between the average TPrP structure (Figure 5) and the average structure of porphine and TPP are evident when the two different pyrroles are compared. This is consistent with the visible absorption spectra which indicate that the aliphatic substitution produces the largest change (Figure 1). The aliphatic substitution appears to have reduced the differences in the bond distances between the two pyrrole rings as indicated in Figure 7. The distances involving the C_α 's of the pyrroles show the largest change in the difference which is a decrease of 0.017 Å; the C_β – C_β' distances show a smaller change of about 0.006 Å which might be significant. Since the former change is closer to the substitution position, the foregoing suggests that the effect decreases as it moves further from the point of substitution. The C–N distances remain essentially the same and this has been noted throughout in the three independent structures.

Finally, the behavior of the bond angles of the two different pyrroles shows that the azapyrrole remains

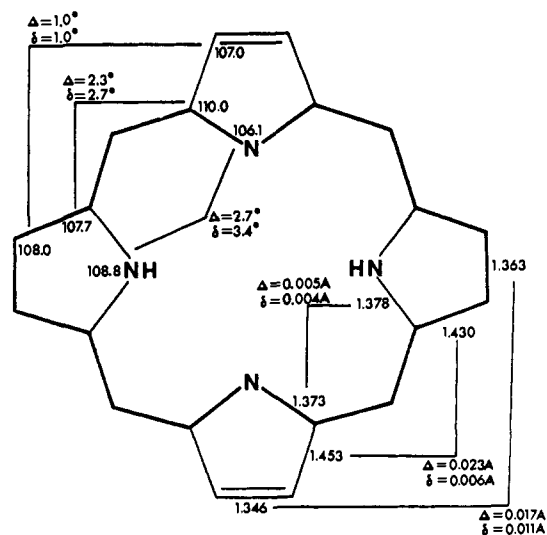


Figure 7. Average structure for porphine and TPP with the differences (Δ) between the pyrrole rings. δ represents the corresponding differences for TPrP.

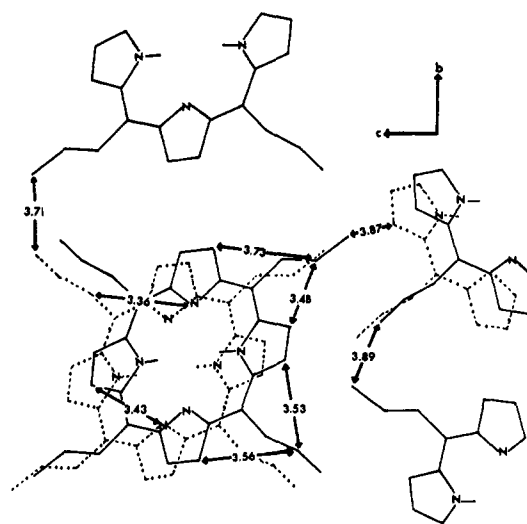


Figure 8. Packing of neighboring TPrP molecules along the a^* directions. Close intra- and intermolecular contact are given (in ångströms).

the same while the reduced pyrrole undergoes changes which cause it to become more different from the azapyrrole than the average difference observed with TPP and porphine (Figure 7). This could be an effect arising from a repulsion of the planar imino hydrogen atoms (Figure 3) which results in increasing the $\angle C_\alpha N C_\alpha'$. The over-all behavior observed with the aliphatic substitution is suggestive of π -electron delocalization onto the side chain.

As with porphine, the deviations of the atoms of TPrP from the NLS plane (Figure 3) are relatively small and the molecule can be considered essentially planar. The pyrrole rings are planar within the error of their determination (Table VI) but the normal to each ring makes a small but definite angle of approximately 2° to the NLS plane. These small tilts are probably related to the manner in which the molecules pack.

The molecules pack in layers along the a^* axis as shown in Figure 8; if the arrangement is viewed per-

pendicular to the molecular planes, one molecule is rotated about the normal to the NLS plane by approximately 45° with respect to the molecule below. This rotation in the stacking arrangement probably results in more space for the side chains; a similar but larger rotation ($\sim 90^\circ$) was found in the packing of TPP.² The stacking is efficient producing a short NB-CP51 intermolecular distance of 3.36 Å, which apparently causes the small tilt observed with pyrrole ring B. The intermolecular distance between NB and CA2 is also short (3.43 Å) and could effect contributions to the tilts of both pyrrole rings. The propyl side chains are in an extended configuration filling the space between the molecules related by the glide plane. One propyl group is rotated about the C_m -CP1 bond producing a short intramolecular contact (3.48 Å) to the adjacent β carbon atom of the pyrrole. This configuration probably arises from a close contact between the methyl carbon atoms, CP63-CP53, in the molecules as they are stacked along b (separation of 3.71 Å, which is short in comparison to the sum of the van der Waals radii for two methyl groups, which is about 4.0 Å). The methyl group on the twisted propyl side chain is also fairly close to the β pyrrole carbon of the adjacent molecule along c (3.87 Å).

The average distance for the C-H bonds is 1.05 ± 0.08 Å; the imino N-H bond length is significantly shorter (0.78 Å). Similar shorter distances for the N-H lengths were observed with TPP (0.96 Å) and porphine (0.86 Å). In contrast to the other structures, the imino hydrogen atom in the TPrP structure is within ± 0.01 Å of the NLS plane and the two \angle CNH angles are essentially the same. However, the shorter N-H bond contributes to give the longest free base H-H distance across the center of the ring: 2.60 Å in TPrP, 2.41 Å in porphine, and 2.36 Å in TPP.

Finally, the relatively short average distance of the CN-CP1 bond (1.522 Å) is probably due to the influence of the sp^2 hybrid bridge carbon atom. However, the second and third atoms of the side chains also show distances shorter than expected. Since it is unlikely that the aromatic character of the macrocycle can affect atoms this remote, the shortening might or might not be real. These atoms have appreciable thermal motion, fairly small peak heights, and the largest expected errors.

Acknowledgment. We would like to take the opportunity here to gratefully acknowledge the support of this work by the National Science Foundation, Molecular Biology Section (Grants GB-5686, GB-7399, and GB-15402).

Mössbauer Studies on Hemin Derivatives of $\alpha,\beta,\gamma,\delta$ -Tetraphenylporphine

Chris Maricondi,¹ Darel K. Straub,* and L. M. Epstein

Contribution from the Department of Chemistry, University of Pittsburgh, Pittsburgh, Pennsylvania 15213. Received May 21, 1971

Abstract: The Mössbauer spectra of $\alpha,\beta,\gamma,\delta$ -tetraphenylporphinatoiron(III) chloride, bromide, iodide, and thiocyanate have been measured at room temperature, 78 and 4.2–6°K. The spectra show a broad asymmetric peak at higher temperatures, which becomes a resolved doublet at 4.2°K. The quadrupole splitting increases in the order chloride < thiocyanate < bromide < iodide.

The hemins are a group of 5-coordinated iron(III) complexes containing a porphyrin dianion and a monodentate anion such as a halide. Hemin itself is (protoporphyrin IX)iron(III) chloride, protoporphyrin IX being the porphyrin occurring in hemoglobin. The hemins have been the subject of numerous Mössbauer studies.^{2–9} Data on isomer shifts and quadrupole splittings obtained much above about 20°K are

quite imprecise because of the unusual broadness and poor peak resolution on the spectra.

We have measured the Mössbauer spectra at 4.2–6°K of [TPPFeCl], [TPPFeBr], [TPPFeI], and [TPPFeSCN], where TPP indicates the $\alpha,\beta,\gamma,\delta$ -tetraphenylporphine dianion. These derivatives were selected in order to determine the effect of the fifth ligand upon isomer shift and quadrupole splitting. In a following paper we will report Mössbauer studies on several $\alpha,\beta,\gamma,\delta$ -tetrakis-(substituted phenyl)porphinatoiron(III) complexes.¹⁰

Experimental Section

The complexes [TPPFeCl], [TPPFeBr], [TPPFeI], and [TPPFeNCS] were prepared as previously described¹¹ using 90% ⁵⁷Fe. Samples for the Mössbauer spectrometer were prepared by powder-

(1) Taken in part from the Ph.D. dissertation of C. Maricondi, University of Pittsburgh, 1969.

(2) L. M. Epstein, *J. Phys. Chem.*, **36**, 2731 (1962).

(3) R. Shulman and G. Wertheim, *Rev. Mod. Phys.*, **36**, 459 (1964).

(4) W. Karger, *Ber. Bunsenges. Phys. Chem.*, **68**, 793 (1964).

(5) V. Gonser and R. W. Grant, *Biophys. J.*, **5**, 823 (1965).

(6) A. J. Bearden, T. H. Moss, W. S. Caughey, and C. A. Beaudreau, *Proc. Nat. Acad. Sci. U.S.A.*, **53**, 1246 (1965).

(7) R. Champion and H. G. Drickamer, *ibid.*, **58**, 876 (1967).

(8) H. Moss, A. J. Bearden, and W. S. Caughey, *J. Chem. Phys.*, **51**, 2624 (1969).

(9) G. Lang, T. Asakura, and T. Yonetani, *Phys. Rev. Lett.*, **24**, 981 (1970).

(10) M. A. Torr ns, D. K. Straub, and L. M. Epstein, *J. Amer. Chem. Soc.*, **94**, 4160 (1972).

(11) C. Maricondi, W. Swift, and D. K. Straub, *ibid.*, **91**, 5205 (1969).